

# Selective Photocatalytic C–C Coupling of Bioethanol into 2,3-Butanediol over Pt-Decorated Hydroxyl-Group-Tunable TiO<sub>2</sub> Photocatalysts

Pengju Yang,<sup>[a, b]</sup> Jianghong Zhao,<sup>\*[a]</sup> Baoyue Cao,<sup>[a, b]</sup> Li Li,<sup>[a]</sup> Zhijian Wang,<sup>[a]</sup> Xuxia Tian,<sup>[a, b]</sup> Suping Jia,<sup>[a]</sup> and Zhenping Zhu<sup>\*[a]</sup>

2,3-Butanediol (2,3-BD) was synthesized through TiO<sub>2</sub>-photocatalytic C–C coupling of bioethanol synchronously with the liberation of an energy H<sub>2</sub> molecule in an anaerobic atmosphere. It was found that the selectivity of 2,3-BD is controlled by the amount of <sup>•</sup>OH. The less the <sup>•</sup>OH, the higher the 2,3-BD selectivity. Furthermore, it was revealed that the amount of <sup>•</sup>OH increases with the increasing of the surface OH groups on TiO<sub>2</sub> photocatalyst. The introduction of water is in favor of the C–C coupling pathway. This can be attributed to the stronger

interaction between water and TiO<sub>2</sub>, which is beneficial to recovering the OH groups and promoting the desorption of <sup>•</sup>CH(OH)CH<sub>3</sub> intermediates, thus suppressing the thermodynamically favorable overoxidation of <sup>•</sup>CH(OH)CH<sub>3</sub> into acetaldehyde and promoting the C–C coupling into 2,3-BD. Based on the findings, the 2,3-BD selectivity was greatly enhanced from approximately 2.6% to approximately 65% over Degussa P25-TiO<sub>2</sub> photocatalyst through fluorine substitution of surface OH groups.

## Introduction

2,3-Butanediol (2,3-BD) is one of the promising bulk chemicals that have a wide range of industrial applications in cosmetics, foods, transport fuels (e.g., as antifreezes, lubricants, or fuel additives), and medicines as well as in the production of polymers (e.g., as resins and synthetic rubber).<sup>[1]</sup> 2,3-BD has three stereoisomeric forms (dextro, levo, and meso isomers), in which the low freezing point of levo isomer (–60 °C) makes it an commercial antifreeze.<sup>[1a, c]</sup> Methyl ethyl ketone (MEK) is the dehydration product of 2,3-BD, which can be used for resins, paints, and other solvents.<sup>[1c]</sup> With a higher burning value than ethanol, MEK is considered as an effective liquid fuel additive.<sup>[1a, 2]</sup> 2,3-BD itself is also a highly valuable fuel with the burning value of 27 198 J g<sup>–1</sup> comparable to other liquid fuels such as ethanol (29 055 J g<sup>–1</sup>) and methanol (22 081 J g<sup>–1</sup>).<sup>[1a]</sup> Owing to its high octane number, 2,3-BD can serve as an “octane booster” for petrol.<sup>[1a]</sup> Through catalytic dehydrogenation, 2,3-BD can be transformed into acetoin and diacetyl, which are flavoring agents used in dairy products, margarines, and cosmetics.<sup>[1a, c, 2]</sup> Further dehydration of 2,3-BD produces 1,3-butadiene, which can be used for synthetic rubber, polyester, and polyurethane.<sup>[1d, 2]</sup> Esterification of 2,3-BD forms the

precursors of polyurethane, which can be used in drugs, cosmetics, lotion, etc.<sup>[1a, e, 2]</sup>

Production of 2,3-BD from biomass would alleviate the dependence on oil sources for platform chemicals. However, 2,3-BD has not been produced on a large scale because of its costly chemical synthesis. Nowadays, commercial production of 2,3-BD is overwhelmingly limited to biofermentation in the context of depleting fossil fuel resources and deteriorating ecological environment because the renewable resource-based biochemicals and biorefineries are sustainable and the microbial production of 2,3-BD had been developed to a commercial scale during World War II.<sup>[1]</sup> Although the fermentation process of 2,3-BD has primarily reached the level of alcohol industry, it has high requirement on environment and bacteria, leading to the high cost of 2,3-BD production (60 000–130 000 yuan t<sup>–1</sup>).<sup>[2]</sup> Therefore, the biofermentation of 2,3-BD has not yet been industrialized and the applications of 2,3-BD developed inadequately up to date. To facilitate the development of 2,3-BD industry, exploring new energy-efficient and atom-economical green synthesis methods is strongly demanded to act as a supplementary and/or an alternative technology to the attractive biosynthesis process.

Photo-driven organic synthesis has been drawing more and more attention in recent years because of its inimitably renewable, green, and mild features in comparison with the conventional synthetic pathways.<sup>[3]</sup> Photochemical and photocatalytic processes are characteristic of reactions among molecules in an electronically excited state, radicals, ions, and/or radical ions, which are significantly different from the ground-state reactions because of the great changes of chemical properties and more particularly of the reactivity of the reactants. They therefore may allow shorter reaction sequences and minimize

[a] Dr. P. Yang, Dr. J. Zhao, Dr. B. Cao, L. Li, Dr. Z. Wang, Dr. X. Tian, Dr. S. Jia, Dr. Z. Zhu

State Key Laboratory of Coal Conversion  
Institute of Coal Chemistry  
Chinese Academy of Sciences  
Taiyuan, 030001 (P.R. China)  
E-mail: zjh\_sx@sxicc.ac.cn

[b] Dr. P. Yang, Dr. B. Cao, Dr. X. Tian  
University of Chinese Academy of Sciences  
Beijing, 100039 (P.R. China)

Supporting Information for this article is available on the WWW under <http://dx.doi.org/10.1002/cctc.201500326>.

undesirable side reactions, thus moving towards the environmental-friendly and atom-economic "green chemistry". Furthermore, photo-driven reactions in many cases involve deep-seated chemical transformations and result in high yields with high selectivity.<sup>[4]</sup> More importantly, photo-driven reactions often follow unique reaction channels and are available of achieving complex, polycyclic or highly functionalized structures from simple substrates<sup>[5a]</sup> and even products that cannot be obtained by conventional ground-state thermal reactions,<sup>[5b]</sup> opening new perspectives in the production of green hydrogen energy<sup>[5c]</sup> and in the search of natural compounds.<sup>[5d]</sup>

2,3-BD is a vicinal diol in which the two hydroxyl groups are bonded to adjacent C2 and C3 carbons, respectively. This unique structure makes it highly difficult to be obtained by the conventional chemical synthesis.<sup>[6]</sup> From the viewpoint of photo-driven organic synthesis, however, 2,3-BD can be achieved by  $\alpha$ -C-C coupling of two  $\alpha$ -hydroxyethyl radicals ( $\cdot\text{CH}(\text{OH})\text{CH}_3$ ) because the radical coupling pathway has shown great interest<sup>[7]</sup> in the photo-driven process for the formation of the C-C bond.<sup>[8]</sup> It was reported in a few pioneering works that the vicinal diols such as ethylene glycol and 2,3-BD were selectively obtained in corresponding methanol and ethanol aqueous solutions by photocatalytic  $\alpha$ -C-C coupling synchronously with  $\text{H}_2$  evolution through water splitting.<sup>[7c,d,9]</sup>  $\text{H}_2$  is a high-energy clean fuel, this method therefore provides a green avenue for synthesizing 2,3-BD in one step especially if the hydrous bioethanol is used as the feedstock. Nevertheless, these reactions have not yet been well developed until recently because the only effective photocatalysts reported were perishable metal sulfide semiconductors (typically  $\text{ZnS}$ )<sup>[7,9]</sup> instead of stable metal oxide semiconductors (e.g.,  $\text{TiO}_2$ ,  $\text{WO}_3$ ,  $\text{ZnO}$ ,  $\text{SnO}_2$ , and so on). Thermodynamically, the higher conduction band edges of metal sulfide are adverse to the injection of an electron from the intermediate radicals by a current-doubling process,<sup>[10]</sup> thus impeding the formation of overoxidation compounds such as aldehydes, acids, and even  $\text{CO}_2$ , but facilitating the C-C coupling reactions.<sup>[11]</sup> Over the metal oxide photocatalysts, the situation is just the opposite.

Recently, through modulating the crystalline structures and pores of  $\text{TiO}_2$ , Lu et al. have found that over  $\text{Pt}/\text{TiO}_2$  photocatalyst ethanol in aqueous solution can be transformed into 2,3-BD with a high selectivity of approximately 97% under UV light irradiation through C-C coupling of  $\cdot\text{CH}(\text{OH})\text{CH}_3$  radicals.<sup>[12]</sup> Simultaneously, a moderate amount of  $\text{H}_2$  was evolved because of the catalytic reduction of protons in the reaction system on the Pt co-catalyst.<sup>[12]</sup> This is contradictory to the above thermodynamic viewpoint and indicates that the reaction pathways over metal oxide photocatalysts can be significantly regulated by changing the adsorption-desorption kinetics and the reaction kinetics. It also shows the possibility of using stable metal oxide photocatalysts to realize the alcohol C-C coupling reactions. In view of the intriguing progress and the wide potential applications of 2,3-BD, it is very urgent to gain more insight into the ways in which how the photocatalytic C-C coupling reaction takes place over the  $\text{Pt}/\text{TiO}_2$  photocatalyst. Especially, the structure-selectivity relationship between  $\text{TiO}_2$  based photocatalyst and C-C coupling per-

formance is of great importance for the further development of photocatalytic 2,3-BD synthesis.

Herein we investigated the C-C coupling of bioethanol over  $\text{Pt}/\text{TiO}_2$  photocatalyst with anatase, rutile, brookite, and anatase-rutile mixed crystalline structures, respectively. It was found that the 2,3-BD selectivity increases significantly with the decreasing of  $\cdot\text{OH}$  content in the reaction system. Moreover, the amount of  $\cdot\text{OH}$  shows a positive correlation with the quantity of surface hydroxyl groups on  $\text{TiO}_2$  photocatalyst, indicating that the oxidative C-C coupling of ethanol may mainly proceed by the  $\cdot\text{OH}$  formed in the reaction between photogenerated holes and surface hydroxyl groups. This was further corroborated over  $\text{Pt}/\text{Degussa-P25-TiO}_2$  photocatalysts through F substitution of surface hydroxyl groups. Water was also found to be in favor of the C-C coupling reaction.

## Results and Discussion

Pure anatase (A-), rutile (R-), brookite (B-)  $\text{TiO}_2$ , and Degussa mixed crystal (P25-)  $\text{TiO}_2$  were incipiently employed to explore the discrepancies in product selectivity in the photocatalytic oxidation of ethanol. In Figure 1, the selectivity of 2,3-BD and overoxidation product (aldehyde, acetic acid,  $\text{CO}$ ,  $\text{CH}_4$ , and  $\text{CO}_2$ ) versus the crystalline phase of  $\text{TiO}_2$  is shown. It is clear that the 2,3-BD selectivity increases in the order of  $\text{Pt}/\text{R-TiO}_2 > \text{Pt}/\text{B-TiO}_2 > \text{Pt}/\text{A-TiO}_2 > \text{Pt}/\text{P25-TiO}_2$ , and the overoxidation product selectivity is on the contrary. This behavior indicates that the formation of 2,3-BD through C-C coupling of ethanol is competitive to the overoxidation of ethanol into aldehyde, acetic acid,  $\text{CO}$ ,  $\text{CH}_4$ ,  $\text{CO}_2$ , and so on. Interestingly, the ethanol conversion decreases from approximately 23% to approximately 5% with the increasing of 2,3-BD selectivity from approximately 2.6% to approximately 85% (Table S1 in the Supporting Information), suggesting the difficulty in obtaining the important purpose of "high selectivity at the high substrate conversion" for catalysis. To find out the causes of the discrepancies in selectivity and activity, some textural and structural characterizations were conducted.

Scanning electron microscopy (SEM) images (Figure 2) exhibit that P25-, A-, and R- $\text{TiO}_2$  are nanoparticles with increasing

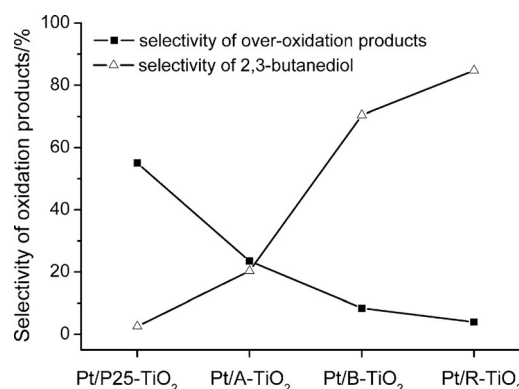


**Figure 1.** Selectivity of 2,3-BD and overoxidation products versus crystalline phase of  $\text{TiO}_2$  over  $\text{Pt}/\text{TiO}_2$  photocatalysts. Reaction conditions: 10 vol% aqueous ethanol solution (200 mL);  $\text{TiO}_2$  decorated with 1 wt% Pt (0.5 g); 300 W high-pressure Hg lamp ( $\lambda = 365$  nm); 24 h; Ar purging.

sizes in the range of 30–300 nm, whereas the B-TiO<sub>2</sub> shows nanoflower morphology constructed by nanorods with diameters of approximately 20–80 nm. X-ray diffraction (XRD) spectra (Figure 3) notarized phase-pure anatase, brookite, and rutile TiO<sub>2</sub> formed. Moreover, the sharp and narrow peaks in XRD spectra together with TEM images (Figure 2) suggest that all of the TiO<sub>2</sub> samples are well crystallized. N<sub>2</sub> adsorption–desorption isotherms (Figure S1 in the Supporting Information) and pore-size distributions (Figure S2) for the TiO<sub>2</sub> samples display that besides the B-TiO<sub>2</sub> having rich mesopores in the range of 3–4 nm, there are relatively fewer pores in P25-, A-, and R-TiO<sub>2</sub>, and the high BET surface area of P25- and A-TiO<sub>2</sub> should be ascribed to their smaller particle sizes (Figure 2).

Note the second highest 2,3-BD selectivity of B-TiO<sub>2</sub>, it seems contradictory to our previous viewpoint<sup>[12]</sup> that the pore structure plays a negative role in the ethanol coupling reaction owing to pore-induced changes in molecular diffusion. As far as is known,<sup>[10–12]</sup> C–C coupling of <sup>•</sup>CH(OH)CH<sub>3</sub> radicals leads to the formation of 2,3-BD, but the <sup>•</sup>CH(OH)CH<sub>3</sub> radicals are thermodynamically facile to be overoxidized on the surface of Pt/TiO<sub>2</sub>. It is therefore crucially important for the ethanol coupling reaction to accelerate the diffusion and desorption of intermediate <sup>•</sup>CH(OH)CH<sub>3</sub> radicals from catalyst surface to bulk liquid. The porous structure was corroborated in our previous work to be detrimental to the ethanol C–C coupling<sup>[12]</sup> because the diffusion of <sup>•</sup>CH(OH)CH<sub>3</sub> radicals from the pore to

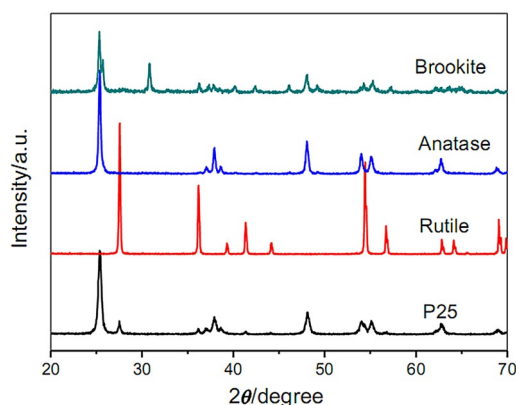


Figure 3. XRD spectra of Degussa P25-, A-, B-, and R-TiO<sub>2</sub>.

the bulk liquid becomes difficult, and the long retention time in the pore should result in further oxidation by additional holes and other oxidizing radicals. The conflict between the high 2,3-BD selectivity and rich porous structure of B-TiO<sub>2</sub> therefore indicates that there should be other unrevealed intrinsic factor controlling the 2,3-BD selectivity, equally important to the phase and pore structures which have been corroborated by solid evidences.<sup>[12]</sup>

UV/Vis spectra (Figure S3) show that the absorption band edge positions of A-, B- and R-TiO<sub>2</sub> samples are located at approximately 400, 380, and 420 nm, respectively, corresponding to the calculated band gaps of 3.1, 3.26, and 2.95 eV, respectively. These values are very close to the reported band gaps of A-, B-, and R-TiO<sub>2</sub>, further confirming phase-pure anatase, brookite, and rutile TiO<sub>2</sub> were obtained.

Surface chemistry was investigated by X-ray photoelectron spectroscopy (XPS). The O 1s XPS spectra of A-, B-, and R-TiO<sub>2</sub> samples (Figure 4) were deconvoluted into two peaks located at binding energies of approximately 529.6 and 531.3 eV, respectively. The former corresponded to bulk O<sup>2-</sup> species, and the latter was ascribed to surface hydroxyl (OH) species.<sup>[13]</sup> Quantification of the O<sup>2-</sup> and OH species shows that the amount of surface OH groups increases in the order of R-TiO<sub>2</sub> < B-TiO<sub>2</sub> < A-TiO<sub>2</sub> < P25-TiO<sub>2</sub> (Figure 5a, Table S2), presenting a negative correlation with the 2,3-BD selectivity (Figure 5b).

Similarly to that of methanol, photocatalytic oxidation of ethanol can proceed through two proposed pathways, namely the direct hole oxidation mechanism and the indirect OH radical (<sup>•</sup>OH) oxidation mechanism.<sup>[14]</sup> Therefore, the <sup>•</sup>OH formed over P25-, A-, B-, and R-TiO<sub>2</sub> was measured by using terephthalic acid (TA) as the trapping agent. By monitoring the photoluminescence (PL) emission spectra of fluorescent 2-hydroxyterephthalic acid (HTA, Figure S4) produced in the reaction between TA and <sup>•</sup>OH (Scheme S1 in the Supporting Information), it was found that the amount of <sup>•</sup>OH formed per minute per gram of TiO<sub>2</sub> increases in the order of R-TiO<sub>2</sub> < B-TiO<sub>2</sub> < A-TiO<sub>2</sub> < P25-TiO<sub>2</sub>, following a similar trend to the amount of surface OH groups versus crystalline phase of TiO<sub>2</sub> (Figure 5a). The positive correlation between PL intensity of HTA and amount of OH groups (Figure 5b) indicates that the <sup>•</sup>OH

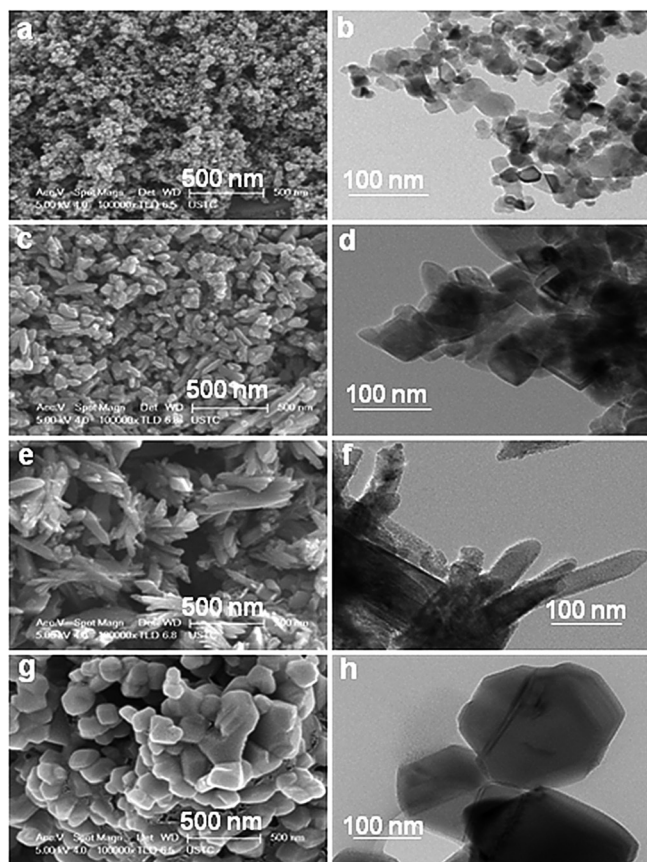


Figure 2. SEM and TEM images of a, b) Degussa P25-; c, d) A-; e, f) B-; and g, h) R-TiO<sub>2</sub>.

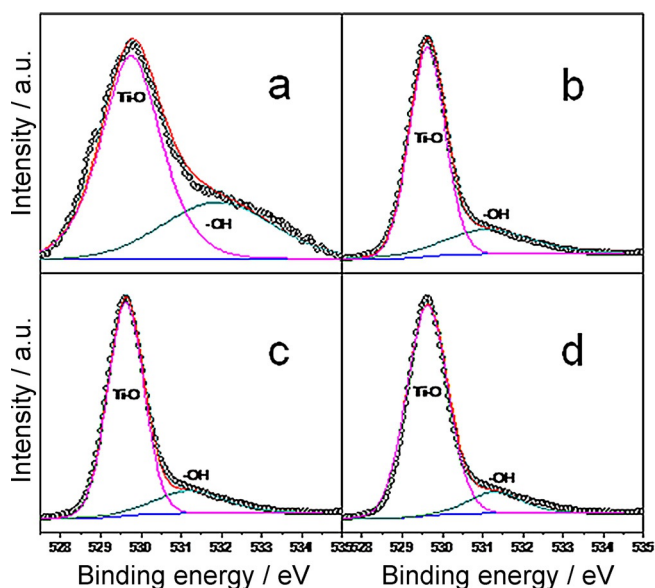


Figure 4. O 1s XPS spectra of a) Degussa P25-, b) A-, c) B-, and d) R-TiO<sub>2</sub>.

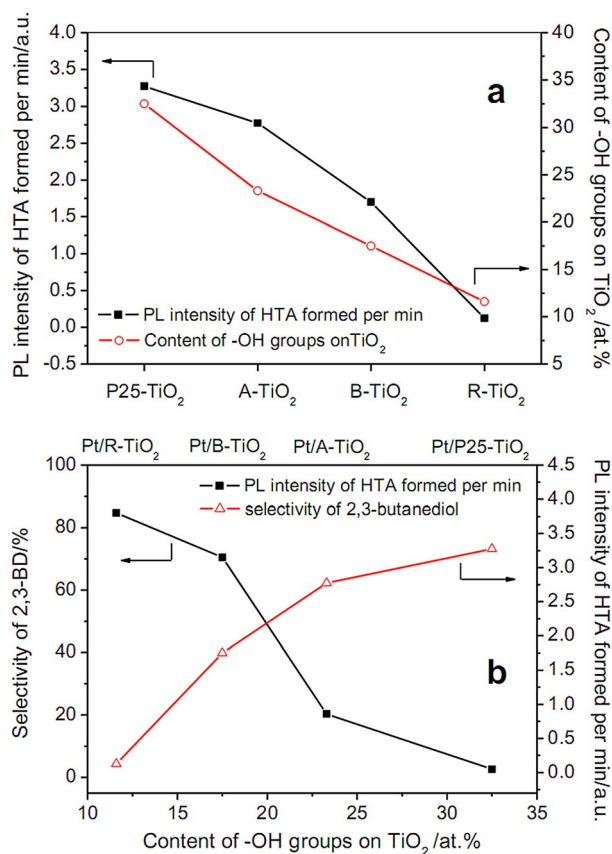


Figure 5. a) PL intensity of HTA formed per minute through the reaction of TA and  $\cdot\text{OH}$  and content of  $-\text{OH}$  groups versus the crystalline phases of TiO<sub>2</sub>; b) PL intensity of HTA formed per minute on TiO<sub>2</sub> and selectivity of 2,3-BD versus content of surface OH groups over Pt-decorated Degussa P25-, A-, B-, and R-TiO<sub>2</sub>.

should be preferentially formed through interfacial reactions between photogenerated holes and surface OH groups, in accordance with those reported in previous studies.<sup>[15]</sup>

It has been corroborated recently that photocatalytic oxidation of pure ethanol over Pt/P25-TiO<sub>2</sub> in an anaerobic atmosphere results in the only product of acetal with a selectivity higher than 99%,<sup>[16]</sup> in which photogenerated holes are the only oxidation species and acetal was produced following a tandem process integrating directly hole-induced alcohol dehydrogenation and in situ H<sup>+</sup>-catalytic acetalation.<sup>[16]</sup> Therefore, the formation of 2,3-BD with a higher selectivity and the disappearance of acetal shown in Table S1 and Table S4 indicate that the reaction pathway of photocatalytic oxidation of ethanol over Pt/TiO<sub>2</sub> was changed greatly if water was involved. The negative correlation between 2,3-BD selectivity and  $\cdot\text{OH}$  shown in Figure 5 clearly suggests that the selectivity of 2,3-BD is preferentially controlled by the  $\cdot\text{OH}$  formed in the reaction system, and the indirect  $\cdot\text{OH}$  oxidation is the reaction mechanism. The results in Figure 5 also show that the less the amount of  $\cdot\text{OH}$ , the higher the 2,3-BD selectivity. More importantly, the  $\cdot\text{OH}$  species produced by interfacial reactions between photogenerated holes and surface OH groups on Pt/TiO<sub>2</sub> photocatalysts (Figure 5 b) implies an efficient way to control the 2,3-BD selectivity through modulating surface OH groups.

Based on these findings, the surface OH groups on commercial P25 mixed-phase TiO<sub>2</sub> were adjusted by fluorine (F) substitution by a simple ligand exchange reaction between F and surface hydroxyl groups on TiO<sub>2</sub> in water (Figure 6 a).<sup>[17]</sup> SEM, TEM, XRD, and UV/Vis characterizations reveal that the morphologies, crystal structures, and light-absorption properties of the F-modified P25-TiO<sub>2</sub> samples remain the same in comparison with original P25-TiO<sub>2</sub> (Figure S5–S7). XPS spectra of the F-modified P25-TiO<sub>2</sub> samples (Figure 6 b) exhibit the characteristic peak of F located at approximately 684.2 eV (inset in Figure 6 b), indicating the substitution of OH groups by F.<sup>[18]</sup> This was corroborated by the O 1s XPS spectra of the F-modified P25-TiO<sub>2</sub> photocatalysts (Figure S8, Table S3), in which the amount of OH groups decreases with the increasing of NaF concentration (Figure 6 c). The photocatalytic performances of Pt/F-P25-TiO<sub>2</sub> photocatalysts presents again that there is a positive correlation between the amount of  $\cdot\text{OH}$  and surface OH groups, and the 2,3-BD selectivity is negatively correlated to the amount of  $\cdot\text{OH}$  in the reaction system (Figure 6 c, Table S4). Notably, over the Pt/F-P25-TiO<sub>2</sub>, the 2,3-BD selectivity was greatly enhanced from approximately 2.6% to approximately 65% through simple F substitution of some of surface OH groups, simultaneously the ethanol conversion as high as approximately 18% was maintained over the F-P25-60 photocatalyst (Table S4).

As discussed above, photocatalytically oxidizing ethanol in water proceeds through the indirect  $\cdot\text{OH}$  oxidation pathway according to Equation (1 a). To selectively convert ethanol into 2,3-BD, the initial  $\cdot\text{CH}(\text{OH})\text{CH}_3$  radicals have to be liberated from the surface of TiO<sub>2</sub> and followed by C–C coupling in the bulk of the solution<sup>[11]</sup> [Eq. (1 b)] because the  $\cdot\text{CH}(\text{OH})\text{CH}_3$  adsorbed on TiO<sub>2</sub> is thermodynamically favorable to inject an additional electron into the conduction band of TiO<sub>2</sub> and easily transform into overoxidized acetaldehyde by a “current doubling” process in the absence of oxygen<sup>[10]</sup> [Eq. (1 c), Figure S9].

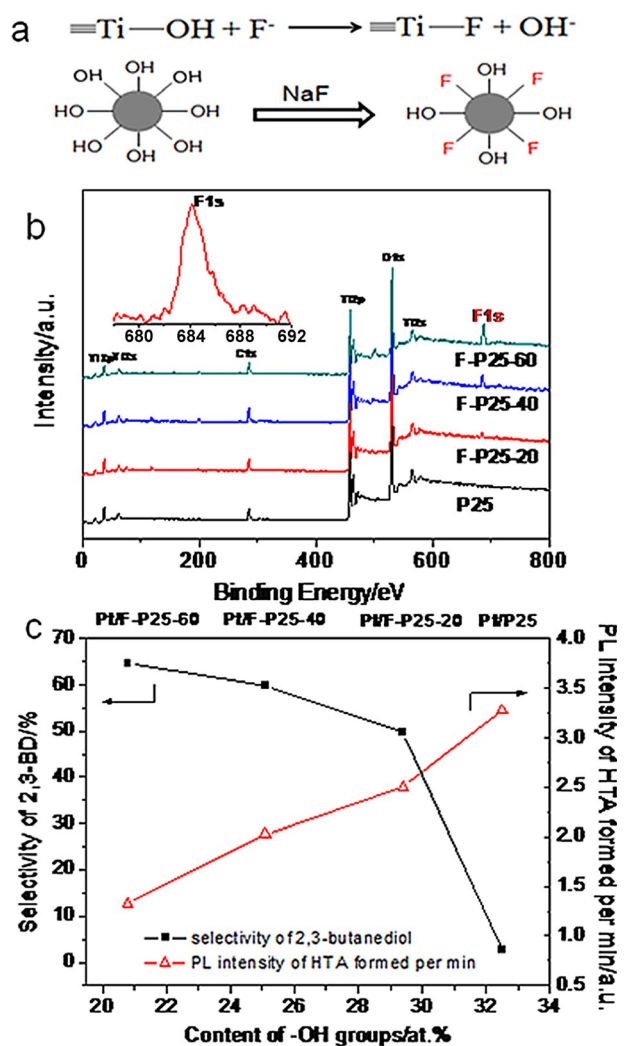
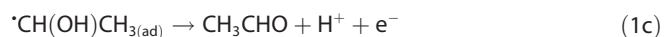
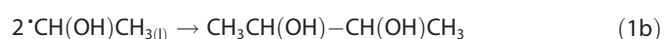


**Figure 6.** a) Schematic illustration of F substitution of hydroxyl groups on TiO<sub>2</sub>; b) XPS spectra of F-modified P25-TiO<sub>2</sub> with varying amount of F, inset is the F 1s XPS spectrum of F-P25-20; c) PL intensity of HTA formed per minute on TiO<sub>2</sub> and selectivity of 2,3-BD versus content of surface OH groups over Pt/F-P25-TiO<sub>2</sub> photocatalysts.



In Figure 7, the electron paramagnetic resonance (EPR) spectra is shown measured during UV light irradiation of P25-TiO<sub>2</sub> in ethanol with and without water. It corroborated the formation of  $\cdot\text{CH}(\text{OH})\text{CH}_3$  intermediate radicals,<sup>[19]</sup> indicating that the first step in photocatalytically oxidizing ethanol is the abstraction of a hydrogen atom from the  $\alpha$ -C-H bond no matter whether water is present or not. According to Equation (1a) to (1c), it is clear that improving the yield of  $\cdot\text{CH}(\text{OH})\text{CH}_3$  in the bulk of the solution is beneficial to C-C coupling, thus leading to higher 2,3-BD selectivity. In Figure 7, UV light irradiation to the aqueous ethanol gave a much stronger EPR spectrum than that in pure ethanol, suggesting more  $\cdot\text{CH}(\text{OH})\text{CH}_3$  produced if water was introduced. As the testing conditions were the

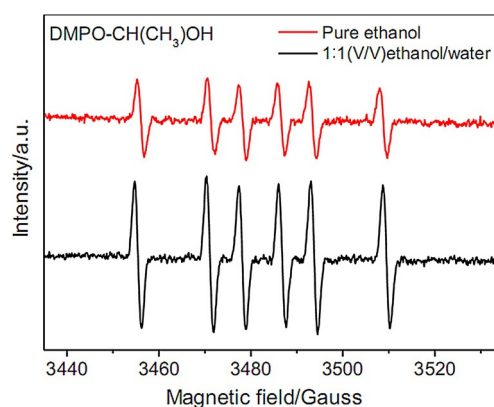


**Figure 7.** EPR spectra of the dimethylpyrroline-N-oxide (DMPO)-P25-TiO<sub>2</sub> system irradiated by UV light in pure ethanol and ethanol aqueous solution ( $V_{\text{ethanol}}/V_{\text{water}} = 1:1$ ).

same, this phenomenon can be explained from the viewpoint of competitive adsorption of water and ethanol on TiO<sub>2</sub>.

Many reports has proved that water and ethanol competitively adsorb on the same surface sites over TiO<sub>2</sub>, although water shows the stronger binding capabilities with respect to ethanol.<sup>[20]</sup> This means that in ethanol aqueous solution, water preferentially adsorbed on TiO<sub>2</sub>. In another words, it is the stronger interaction between water and TiO<sub>2</sub> that is in favor of promoting the desorption of  $\cdot\text{CH}(\text{OH})\text{CH}_3$  intermediates, thus suppressing the overoxidation of  $\cdot\text{CH}(\text{OH})\text{CH}_3$  into acetaldehyde by the current doubling process and promoting the C-C coupling into 2,3-BD. Furthermore, water is beneficial to recovering the OH groups, which can undoubtedly maintain the formation of  $\cdot\text{OH}$  and improve the 2,3-BD selectivity. With regard to the high ethanol conversion of approximately 18% over Pt/F-P25-60 (Table S4) compared to that of approximately 5% over pure-phase Pt/R-TiO<sub>2</sub> (Table S1), the high activity of Pt/F-P25-60 should be originated from the anatase-rutile hybridized TiO<sub>2</sub> structure of Degussa P25, which is well-known to be able to effectively improve electron-hole separation.<sup>[21]</sup>

The reaction mechanism proposed above suggests that water should play a very important role in tuning the ethanol oxidation pathways in the anaerobic photocatalytic system. This is significantly important to the synthetic systems containing water from the practical point of view, especially in which water is very difficult to be separated. For example, dewatering of bioethanol is one of the most energy-intensive procedures in the industrial processes for the conversion of bioethanol.<sup>[22]</sup> In Figure 8, the selectivity of 2,3-BD over the Pt/R-TiO<sub>2</sub> versus ethanol volume fraction in water is shown. Clearly the 2,3-BD selectivity increases significantly from 25% to 60% if only 2.5 vol% water was introduced into the photocatalytic system. Afterwards, water shows an increasingly improving effect on the selectivity of C-C coupling over the Pt/R-TiO<sub>2</sub> photocatalysts in a wide range of  $V_{\text{ethanol}}/V_{\text{water}}$  ratios. If the  $V_{\text{ethanol}}/V_{\text{water}}$  ratio is higher than 60:140, however, the 2,3-BD selectivity decreases.

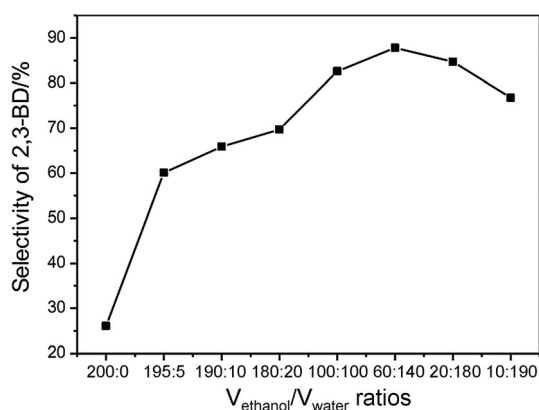


**Figure 8.** Selectivity of 2,3-BD over Pt/R-TiO<sub>2</sub> versus ethanol volume fraction in water. Reaction conditions: 10 vol% aqueous ethanol solution (200 mL); TiO<sub>2</sub> (0.5 g) decorated with 1 wt% Pt; 300 W high-pressure Hg lamp ( $\lambda = 365$  nm); 24 h; Ar purging.

## Conclusions

It was found that photocatalytic C–C coupling of ethanol into 2,3-butanediol (BD) in the anaerobic conditions over Pt/TiO<sub>2</sub> photocatalysts is controlled by the amount of  $\cdot\text{OH}$  in the reaction system. The amount of  $\cdot\text{OH}$  can be tuned by the quantity of surface OH groups on the TiO<sub>2</sub> photocatalyst because the  $\cdot\text{OH}$  radicals are produced by the reaction of the photogenerated holes with the surface OH groups. Based on the findings, the 2,3-BD selectivity was greatly enhanced from approximately 2.6% to approximately 63% over commercial Pt/P25-TiO<sub>2</sub> photocatalysts through simple F substitution of some of the surface OH groups on P25-TiO<sub>2</sub>, and the ethanol conversion as high as approximately 18% was maintained over the Pt/F-P25-60 photocatalyst. More importantly, the introduction of water can promote the C–C coupling reactions greatly. The work provides a novel avenue for the upgrading of bioethanol without the energy-intensive dewatering procedures. Furthermore, this would also open a wide way for the green and energy-efficient transformation and utilization of biomass through employing bioethanol as the platform molecule.

## Experimental Section

### Catalyst preparation

R-TiO<sub>2</sub> was prepared by calcination of commercial P25 in a muffle furnace in air at 800 °C for 8 h. A-TiO<sub>2</sub> was prepared by a hydrothermal method. Typically, diethylene glycol (5 mL), tetrabutyl titanate (5 mL), and 10% tetrabutyl ammonium hydroxide (20 mL) were mixed and then magnetically stirred for 30 min at RT. The mixed solution was then transferred to a Teflon-lined stainless-steel autoclave and heated for 24 h at 200 °C. B-TiO<sub>2</sub> were prepared by a hydrothermal method, too. Tetrabutyl titanate (7.8 mL) was directly hydrolyzed in a solution of sodium chloride (1.10 g) and aqueous ammonia (NH<sub>3</sub>·H<sub>2</sub>O, 68 mL). After stirring for a short time, the resulting suspension was transferred to a Teflon-lined stainless-steel autoclave and heated to 180 °C for 24 h.

The F-modified P25-TiO<sub>2</sub> was prepared by soaking commercial P25-TiO<sub>2</sub> in 20, 40, and 60 mM NaF aqueous solution (pH  $\approx$  3.5 by

HCl regulation) for 3 h, respectively, then dried at 80 °C. The samples were denoted as F-P25-20, F-P25-40, and F-P25-60, respectively.

### Catalyst characterization

Phase structure of the TiO<sub>2</sub> photocatalysts was examined by XRD using a BRUKER D8 Advance X-ray diffractometer with Cu<sub>K $\alpha$</sub>  radiation ( $\lambda = 0.15406$  nm) operating at 40 kV. SEM was performed on a JEOL JSM-6700F microscope operating at 5 kV. TEM images were obtained on a JEOL JEM-2010 microscope with an accelerating voltage of 200 kV. UV/Vis absorption spectra were recorded on a Shimadzu UV 3600 UV/Vis/NIR spectrophotometer. XPS was performed on a Thermo ESCALAB 250 XPS spectrometer with Al<sub>K $\alpha$</sub>  ( $h\nu = 1486.6$  eV) radiation. To eliminate the effect of sample surface charging on the shift of XPS peak of carbon, the C1s reference of 284.5 eV was chosen for the calibration of binding energy. EPR spectra of DMPO-CH(CH<sub>3</sub>)OH were measured by an ESP300E EPR spectrometer at RT. The mixture containing TiO<sub>2</sub> (5 mg), spin-trap DMPO (20  $\mu\text{L}$ , 0.2 M) and ethanol aqueous solution (100  $\mu\text{L}$ ) was transferred to a quartz capillary and oxygen in the quartz capillary was removed by nitrogen purging. Afterwards, the mixture solution was irradiated by UV light source (355 nm) to generate  $\cdot\text{CH}(\text{OH})\text{CH}_3$ .

### Photocatalytic measurements

10 vol% Ethanol aqueous solution (200 mL) and TiO<sub>2</sub> (0.5 g) of containing 1 wt% Pt were employed to perform the photocatalytic measurements in anaerobic conditions. 300 W high-pressure Hg lamp ( $\lambda = 365$  nm) was used as the light source. During the reaction, both gaseous and liquid products were analyzed using gas chromatography (GC) and GC-MS coupling.

$\cdot\text{OH}$  radicals in the reaction system were measured by the TA fluorescence probe method as follows. TiO<sub>2</sub> powder samples of 0.1 g were dispersed in 100 mL of  $5 \times 10^{-4}$  M TA aqueous solution with a concentration of  $2 \times 10^{-3}$  M NaOH. Then the measurements were performed under UV light irradiation using a 300 W high-pressure Hg lamp. PL spectra of luminescent HTA were obtained on a Hitachi F-7000 fluorescence spectrophotometer excited by 315 nm light.

Photocatalytic performances were mainly investigated by the product selectivity, which was defined as the molar percentage of ethanol converted into the specific products according to chemical formula in the total moles of ethanol converted. For example,  $2 \text{CH}_3\text{CH}_2\text{OH} \rightarrow \text{CH}_3\text{CH}(\text{OH})-\text{CH}(\text{OH})\text{CH}_3$ , then the 2,3-BD selectivity was calculated by using the following formula:

$$\text{Selectivity of 2,3-BD} = \frac{\text{Molar amount of 2,3-BD} \times 2}{\text{Total molar amount of ethanol converted}}$$

### Acknowledgements

This work was supported by the National Natural Science Foundation of China (21173250), the Knowledge Innovation Project of Chinese Academy of Sciences (KG CX2-EW-311), and the Innovation Project of Institute of Coal Chemistry, Chinese Academy of Sciences for Preeminent Youth (2011SQNRC19).

**Keywords:** alcohols · biomass · C–C coupling · photochemistry · titanates

- [1] a) X.-J. Ji, H. Huang, P.-K. Ouyang, *Biotechnol. Adv.* **2011**, *29*, 351; b) E. Celińska, W. Grajek, *Biotechnol. Adv.* **2009**, *27*, 715; c) S. K. Garg, A. Jain, *Bioresour. Technol.* **1995**, *51*, 103; d) A.-P. Zeng, W. Sabra, *Curr. Opin. Biotechnol.* **2011**, *22*, 749; e) X.-J. Ji, H. Huang, J. Du, J.-G. Zhu, L.-J. Ren, S. Li, Z.-K. Nie, *Bioresour. Technol.* **2009**, *100*, 5214; f) M. J. Syu, *Appl. Microbiol. Biotechnol.* **2001**, *55*, 10.
- [2] L. Ge, X. Wu, J. Chen, J. Wu, *J. Biomater. Nanobiotechnol.* **2011**, *2*, 335–336.
- [3] a) G. Palmisano, V. Augugliaro, M. Pagliarob, L. Palmisano, *Chem. Commun.* **2007**, 3425–3437; b) D. Ravelli, D. Dondi, M. Fagnoni, A. Albin, *Chem. Soc. Rev.* **2009**, *38*, 1999–2011.
- [4] H. Kisch, *Angew. Chem. Int. Ed.* **2013**, *52*, 812–847; *Angew. Chem.* **2013**, *125*, 842–879.
- [5] a) A. Maldotti, A. Molinari, *Photocatalysis*, Springer, Verlag Berlin Heidelberg, **2011**, pp. 185; b) N. Hoffmann, *Chem. Rev.* **2008**, *108*, 1052–1103; c) X. Chen, S. Shen, L. Guo, S. S. Mao, *Chem. Rev.* **2010**, *110*, 6503–6570; d) T. Bach, J. P. Hehn, *Angew. Chem. Int. Ed.* **2011**, *50*, 1000–1045; *Angew. Chem.* **2011**, *123*, 1032–1077.
- [6] a) E. N. Jacobsen, I. Marko, W. S. Mungall, G. Schroeder, K. B. Sharpless, *J. Am. Chem. Soc.* **1988**, *110*, 1968–1970; b) H. C. Kolb, M. S. VanNieuwenhze, K. B. Sharpless, *Chem. Rev.* **1994**, *94*, 2483–2547.
- [7] a) P. Johnne, H. Kisch, *J. Photochem. Photobiol. A* **1997**, *111*, 223–228; b) G. Hörner, P. Johnne, R. Kunneth, G. Twardzik, H. Roth, T. Clark, H. Kisch, *Chem. Eur. J.* **1999**, *5*, 208–217; c) L. H. Chen, W. Z. Gu, X. W. Zhu, F. D. Wang, Y. Z. Song, J. H. Hu, *J. Photochem. Photobiol. A* **1993**, *74*, 85–89; d) L. H. Chen, X. W. Zhu, F. D. Wang, W. Z. Gu, *J. Photochem. Photobiol. A* **1993**, *73*, 217–220.
- [8] M. Fagnoni, D. Dondi, D. Ravelli, A. Albin, *Chem. Rev.* **2007**, *107*, 2725–2756.
- [9] S. Yanagida, T. Azuma, H. Kawakami, H. Kizumoto, H. Sakurai, *J. Chem. Soc. Chem. Commun.* **1984**, 21–22.
- [10] a) M. Miyake, H. Yoneyama, H. Tamura, *Chem. Lett.* **1976**, 635–640; b) S. Yamagata, S. Nakabayashi, K. M. Sancier, A. Fujishima, *Bull. Chem. Soc. Jpn.* **1988**, *61*, 3429–3434.
- [11] a) B. R. Müller, S. Majoni, D. Meissner, R. Memming, *J. Photochem. Photobiol. A* **2002**, *151*, 253–265; b) B. R. Müller, S. Majoni, R. Memming, D. Meissner, *J. Phys. Chem. B* **1997**, *101*, 2501–2507.
- [12] H. Lu, J. Zhao, L. Li, L. Gong, J. Zheng, L. Zhang, Z. Wang, J. Zhang, Z. Zhu, *Energy Environ. Sci.* **2011**, *4*, 3384–3388.
- [13] a) B. Erdem, R. A. Hunsicker, G. W. Simmons, E. D. Sudol, V. L. Dimonie, M. S. El-Aasser, *Langmuir* **2001**, *17*, 2664; b) J. Yu, H. Yu, B. Cheng, M. Zhou, X. Zhao, *J. Mol. Catal. A* **2006**, *253*, 112; c) E. McCafferty, J. P. Wightman, *Surf. Interface Anal.* **1998**, *26*, 549.
- [14] J. Schneider, D. W. Bahnemann, *J. Phys. Chem. Lett.* **2013**, *4*, 3479–3483.
- [15] a) R. I. Bickley, V. Vishwanathan, *Nature* **1979**, *280*, 306–308; b) C. S. Turchi, D. F. Ollis, *J. Catal.* **1990**, *122*, 178–192; c) J. Chen, D. F. Ollis, W. H. Rulkens, H. Bruning, *Water Res.* **1999**, *33*, 669–676.
- [16] H. Zhang, Z. Zhu, Y. Wu, T. Zhao, L. Li, *Green Chem.* **2014**, *16*, 4076–4080.
- [17] a) C. Minero, G. Mariella, V. Maurino, E. Pelizzetti, *Langmuir* **2000**, *16*, 2632–2641; b) J. S. Park, W. Choi, *Langmuir* **2004**, *20*, 11523–11527.
- [18] a) H. Park, W. Choi, *J. Phys. Chem. B* **2004**, *108*, 4086–4093; b) H. G. Yang, C. H. Sun, S. Z. Qiao, J. Zou, G. Liu, S. C. Smith, H. M. Cheng, G. Q. Lu, *Nature* **2008**, *453*, 638–641.
- [19] a) G. R. Buettner, *Free Radical Biol. Med.* **1987**, *3*, 259–303; b) E. Finkelstein, G. M. Rosen, E. J. Rauckman, *Arch. Biochem. Biophys.* **1980**, *200*, 1–16; c) R. Dunford, E. J. Land, M. Rozanowska, T. Sarna, T. G. Truscott, *Free Radical Biol. Med.* **1995**, *19*, 735–740.
- [20] a) S. Pilkenton, S. J. Hwang, D. Raftery, *J. Phys. Chem. B* **1999**, *103*, 11152–11160; b) C. Y. Wang, H. Groenzin, M. J. Shutz, *J. Am. Chem. Soc.* **2004**, *126*, 8094–8095.
- [21] a) T. Ohno, K. Sarukawa, K. Tokieda, M. Matsumura, *J. Catal.* **2001**, *203*, 82; b) D. C. Hurum, A. G. Agrios, K. A. Gray, *J. Phys. Chem. B* **2003**, *107*, 4545.
- [22] a) H. Shapouri, J. A. Duffield, M. Wang, *The Energy Balance of Corn Ethanol: An Update* (report no. 814, Office of the Chief Economist, U. S. Department of Agriculture, **2002**; available at [www.usda.gov/oce/oepnu/aer-814.pdf](http://www.usda.gov/oce/oepnu/aer-814.pdf)); b) G. W. Huber, J. N. Chheda, C. J. Barrett, J. A. Dumesic, *Science* **2005**, *308*, 1446; c) S. I. Mussatto, G. Dragone, P. M. R. Guimarães, J. P. A. Silva, L. M. Carneiro, I. C. Roberto, A. Vicente, L. Domingues, J. A. Teixeira, *Biotechnol. Adv.* **2010**, *28*, 817.

Received: March 26, 2015

Published online on June 24, 2015